A de novo X;8 translocation creates a PTK2-THOC2 gene fusion with THOC2 expression knockdown in a patient with psychomotor retardation and congenital cerebellar hypoplasia

UNIVERSITÀ DEGLI STUDI DI TORINO

A *de novo* X;8 translocation creates a *PTK2-THOC2* gene fusion with *THOC2* expression knockdown in a patient with psychomotor retardation and congenital cerebellar hypoplasia

Eleonora Di Gregorio[1,2], Federico T. Bianchi[3], Alfonso Schiavi[4,5], Alessandra M.A. Chiotto[3], Marco Rolando[6], Ludovica Verdun di Cantogno[7], Enrico Grosso[2], Simona Cavalieri[2] , Alessandro Calcia[1], Daniela Lacerenza[1], Orsetta Zuffardi[8,9],Saverio Francesco Retta[10], Giovanni Stevanin[11,12], Cecilia Marelli[11,12], Alexandra Durr[11,12], Sylvie Forlani[11], Jamel Chelly[13], Francesca Montarolo[14], Filippo Tempia[14], Hilary E. Beggs[15], Robin Reed[16], Stefania Squadrone[17], Maria C. Abete[17], Alessandro Brussino[1], Natascia Ventura[4,5], Ferdinando Di Cunto[3], and Alfredo Brusco[1,2*]

[1] University of Torino, Department of Medical Sciences, Italy

[2] S.C.d.U. Medical Genetics, Città della Salute e della Scienza, Torino, Italy

[3] University of Torino, Department of Molecular Biotechnology and Health Sciences, Molecular Biotechnology Centre, Via Nizza 52, 10126, Torino, Italy.

[4] University of Roma "Tor Vergata", Department of Biomedicine and Prevention, Italy

[5] Institute of Clinical Chemistry and Laboratory Medicine of the Heinrich Heine University, and the IUF - Leibniz Research Institute for Environmental Medicine, Duesseldorf, Germany

[6] S.C. Neuropsichiatria Infantile, ASL TO3, Pinerolo, Italy

[7] S.C.d.U. Anatomia Patologica, Città della Salute e della Scienza, Torino, Italy

[8] Department of Molecular Medicine, University of Pavia, Pavia, Italy

[9] IRCCS "National Neurological Institute C. Mondino" Foundation, Pavia, Italy

[10] Department of Clinical and Biological Sciences, University of Turin, Orbassano, Italy

[11] Centre de Recherche de l'Institut du Cerveau et de la Moelle épinière (INSERM / UPMC Univ. Paris 6, UMR_S975 ; CNRS 7225, EPHE), Pitié-Salpêtrière Hospital, Paris, France

[12] APHP, Fédération de génétique, Pitié-Salpêtrière Hospital, Paris, France

[13] Université Paris Descartes, Institut Cochin - Hôpital Cochin, Paris - France

[14] University of Torino, Neuroscience Institute Cavalieri Ottolenghi (NICO), Torino, Italy

[15] Department of Ophthalmology, University of California San Francisco, San Francisco, CA 94122, USA

[16] Department of Cell Biology, Harvard Medical School, Boston, USA

[17] Istituto Zooprofilattico Sperimentale del Piemonte, Liguria e Valle d'Aosta, CReAA- National Reference Centre for Surveillance and Monitoring of Animal Feed, Lab. Contaminanti Ambientali,

Torino, Italy

* Corresponding author: Alfredo Brusco, Department of Medical Sciences University of Torino, via Santena, 19 - 10126 Torino, Italy. Fax: +39 011 670 5668; *e-mail:* alfredo.brusco@unito.it

Keywords: chromosomal translocation; PTK2; FAK; THOC2; cerebellar hypoplasia

Running head: *THOC2, PTK2* and cerebellar hypoplasia

Conflict of interest: The authors declare no conflict of interest

Word count: 3781

ABSTRACT

We identified a balanced *de novo* translocation involving chromosomes Xq25 and 8q24 in an eight year-old girl with a non-progressive form of congenital ataxia, cognitive impairment and cerebellar hypoplasia. Breakpoint definition showed that the promoter of the *Protein Tyrosine Kinase 2* (*PTK2*, also known as *Focal Adhesion Kinase, FAK*) gene on chromosome 8q24.3 is translocated 2 kb upstream of the THO complex subunit 2 (*THOC2*) gene on chromosome Xq25. *PTK2* is a well-known non-receptor tyrosine kinase whereas *THOC2* encodes a component of the evolutionarily conserved multiprotein THO complex, involved in mRNA export from nucleus. The translocation generated a sterile fusion transcript under the control of the *PTK2* promoter, affecting expression of both *PTK2* and *THOC2* genes. PTK2 is involved in cell adhesion and, in neurons, plays a role in axonal guidance, and neurite growth and attraction. However, *PTK2* haploinsufficiency alone is unlikely to be associated with human disease. Therefore, we studied the role of THOC2 in the CNS using three models: 1) *THOC2* ortholog knockout in *C.elegans* which produced functional defects in specific sensory neurons; 2) *Thoc2* knockdown in primary rat hippocampal neurons which increased neurite extension; 3) *Thoc2* knockdown in neuronal stem cells (LC1) which increased their in vitro growth rate without modifying apoptosis levels. We suggest that *THOC2* can play specific roles in neuronal cells and, possibly in combination with *PTK2* reduction, may affect normal neural network formation, leading to cognitive impairment and cerebellar congenital hypoplasia.

INTRODUCTION

Cerebellar malformations are rare developmental disorders that comprise many heterogeneous diseases, with both acquired and genetic causes [1]. They can be confined to the cerebellum or variably involve other infratentorial or supratentorial structures, such as the brainstem, the corpus callosum and the cerebral cortex [2]. The cerebellum is usually hypoplastic, at difference from neurodegenerative disorders, in which progressive cerebellar atrophy is observed.

Nevertheless, the distinction between cerebellar hypoplasia and cerebellar atrophy is not always clear-cut, as secondary atrophy may occur in a hypoplastic cerebellum. Both syndromic and pure forms of cerebellar hypoplasia are known. The clinical spectrum associated with cerebellar hypoplasia varies according to the aetiology, and includes non-progressive congenital ataxia (NPCA), abnormal ocular movements and, less frequently, hypotonia. Besides motor deficits, clinical features may include developmental delay, cognitive impairment, deficit of executive functions, language deficits, and mood disorders including autistic-like behaviour [3]. The genetic component has been partially defined in recent years, and autosomal recessive, autosomal dominant or X-linked inheritance have been reported (http://neuromuscular.wustl.edu/ataxia/recatax.html#congenital). At least 15 syndromes with cerebellar hypoplasia have X-linked inheritance. For some of them causative genes have been identified (e.g. *OPHN1, DKC1, CASK* and *CUL4B)* [4, 5], while two additional loci have been mapped to Xp11.21-Xq24 [6, 7] and Xq25-q27.1 [8], respectively.

Here we report the detailed investigation, starting from the abnormal karyotype, in a child affected by cerebellar hypoplasia, non-progressive congenital ataxia, and psychomotor delay. Cytogenetic and breakpoint analyses led to the identification of genes potentially involved in the disease, a role corroborated by functional analyses.

MATERIALS AND METHODS

Subjects, cell lines, and extraction of genomic DNA and total RNA

Peripheral blood lymphocytes (PBL) were obtained from the patient and her parents. PBL were used to create immortalized lymphoblastoid cell lines (LCL) by Epstein-Barr Virus (EBV) transformation. Fibroblasts were obtained from dermal biopsy of the patient and three healthy gender-matched adult controls. Informed consent was obtained for the patient and her parents. Genomic DNA was extracted from peripheral blood (Qiagen, Hilden, Germany) following the manufacturer's instructions. Total RNA was extracted from lymphoblasts or fibroblasts using an RNeasy Plus Mini Kit (Qiagen), and retro-transcribed using the

Transcriptor First Strand cDNA Synthesis kit (Roche Diagnostics, Mannheim, Germany).

Cytogenetic, Fluorescence In Situ Hybridization (FISH) analyses, array-CGH

Cytogenetic analysis of peripheral blood lymphocytes from the proband and both parents was performed using standard techniques. Array-CGH was carried out on genomic DNA using a whole genome oligonucleotide microarray platform (Human Genome CGH Microarray 244A Kit; Agilent Technologies, Santa Clara, California, USA) (see the supplement).

Mice tissue collection and RNA isolation

Thoc2 and *Ptk2* mRNA quantification was performed on tissues obtained from C57BL/6 mice at different ages from embryonic day 14 (E14) to two months postnatal (P60), including the day of birth (P0) (pools of three individuals per time point) (see the supplement).

In vitro transcription/translation

To obtain the chimeric *PTK2-THOC2* transcript, we amplified the patient's cDNA using a forward primer on exon 1 of the *PTK2* gene and a reverse primer on exon 12 of the *THOC2* gene. Transcription/translation was performed using TnT T7 Quick for PCR as described (Promega) (see the supplement).

Caenorhabditis elegans models, *nematode strains, maintenance and gene silencing*.

Strains utilized in this work were N2:wild type Bristol, RB776: *kin-32*(ok166) I, and VC673: *thoc-2*(ok961) III/hT2[bli-4(e937) let-?(q782) qIs48] (I;III). We employed standard nematode culture conditions [9]. Strains were maintained at 20ºC on Nematode Growth Media agar supplemented with *Escherichia coli* (OP50 or transformed HT115). Gene silencing was carried out through the RNA interference feeding technique as previously described [10] using bacteria transformed with L4440 empty vector as control, or L4440 containing dsRNA against *kin-32* (C30F8.4), or *thoc-2* (C16A3.8). Functional assays were performed as described in the supplement.

PTK2 expression induction

Patient's fibroblast cells ($2x10^4$) were plated on 24-well plates, cultured overnight, treated with 50 ng/ml of TNF-alpha (p.n. T6674, Sigma-Aldrich, St. Louis, MO, USA) for 6 h. Total RNA was collected using the Cells-to-Ct kit (Applied Biosystem) according to the manufacturer's protocols. Messanger RNA levels of *PTK2*, *PTK2-THOC2* fusion product and *THOC2* were determined by real-time RT-PCR as described in the supplement.

Rat hippocampal neurons and LC1 neuronal precursors culture and silencing

Primary cultures of rat hippocampal neurons were prepared from rat embryonic brains at E17.5 as previously described [9]. For morphological analysis in the first stages of development, $5 \cdot 10^5$ neurons were nucleofected with Amaxa Nucleofection Kit (Lonza, Cologne, Germany). Neurons were plated in MEM-Horse medium on poly-L-lysine pre-coated coverslips. After 4 hours, medium was changed in N2 medium and coverslips were flipped upside down. For morphological analysis $2 \cdot 10^5$ neurons were plated.

LC1 were plated (typically $2–3 \cdot 10^6$ cells into a T75 flask) on uncoated plastic in Neuromed N medium (Euroclone, Milan, Italy) supplemented with modified N2 [10] and 10 ng/ml of both EGF and FGF-2 (NS expansion medium). LC1 were detached with Accutase (Invitrogen), pelleted in PBS and then split into fresh plates. For transfection $8 \cdot 10^6$ cells were nucleofected with Amaxa Nucleofection Kit.

For transfection in hippocampal neurons and LC1 we used two efficient *Thoc2* siRNA constructs (Sh8137 and Sh2113, Ambion).

Rat hippocampal neurons grown on coverslips were fixed with 4% paraformaldehyde (PFA) / PBS for 10 minutes, then quenched with NH_4Cl 50 mM / PBS. Permeabilization was performed with 0.1% TritonX-100 / PBS for 3 minutes and a 5% BSA/PBS saturation was left for 30 minutes over the coverslips. Following this step, primary antibodies were left for 1 hour and appropriate Alexa-conjugated secondary antibodies were used for 30 minutes followed by other three washings with PBS. Coverslips were mounted with Mowiol on cover glasses and analyzed with an inverted fluorescence microscope. All samples were examined using Apotome system (Zeiss).

The following primary antibodies were used: mouse monoclonal anti-SMI 312 (Covance), mouse monoclonal anti-alpha Tubulin (Sigma); counterstaining using Phalloidin (Sigma) for actin and DAPI (Sigma) for nuclei was used.

Further Materials and Methods are in the Supplement.

RESULTS

Clinical, neuroradiological, biochemical and genetic analyses

The patient was born after an uneventful pregnancy. No problems were reported at birth, in the perinatal period, and during the first year of life. Symptoms were noted at ~15 months when she started walking, and consisted of motor incoordination and unsteady gait. Brain magnetic resonance imaging (MRI) at 23 months revealed hypoplasia of the cerebellar hemispheres and vermis. MRI was repeated at ~ 6 yrs and corfirmed hypoplasia of the posterior fossa with low-set tentorium, not progressive over time. Both cerebellar hemispheres and vermis were hypoplastic with enlargement of the IV ventricle (Fig. 1A and supplemental Fig. 1).

At 8 yrs the patient underwent detailed clinical investigation: electrocardiogram was normal; mild dysmorphic features were noted: joint hypermobility, micrognathia leading to malocclusion, ogival palate, pointed chin, low-set and protruding ears, small hands (10^{th} centile) with tapering fingers and clinodactyly of the 4^{th} finger, hyperconvex toenails.
Neurological features included gait and limb ataxia, dysmetria, adiadochokinesia and diffuse hypothonia. The patient also presented with bradylalia, dysarthria, occasional dyslalia and pneumophonic coordination impairment. Babinski sign was present on the left foot only; osteotendinous reflexes were weak at the four limbs. Eye movements were normal and nystagmus was absent. Mild intellectual disability was present, with impaired visual and spatial orientation. Moreover, aggressive behavior and socially inappropriate and derogatory remarks (coprolalia) were reported. Biochemical blood analyses were normal. Serum alpha-fetoprotein was within normal range. Sialoglycoprotein deficits were ruled out by laboratory testing. Friedreich's ataxia was excluded by routine genetic testing.

Cytogenetic analysis

Chromosome analysis found a translocation involving chromosomes X and 8: 46,X,t(X;8)(q25;q24.3) (Fig. 1B). The normal karyotype of the parents and the segregation of polymorphic markers (Profiler Plus kit, Applied Biosystems) demonstrated that the translocation was *de novo*. FISH analysis with probes painting the X chromosome confirmed the translocation (data not shown), and a subtelomeric 8q probe (Vysis) proved that a small telomeric 8q region was translocated on the der(X) chromosome. Array-CGH analysis using a 244 K array (Agilent Technologies) did not reveal genomic deletion/duplication besides a few known copy number variants.

X-inactivation was completely skewed in the proband (see the supplement, fig. 1C), with the active allele inherited from the father.

Mapping and characterization of the breakpoint junctions

We mapped the breakpoint to a region of ~ 37 kb and defined the translocation between 8q24.3 and Xq25 by FISH (Fig.1D and 1E; details in the supplement).

We used a set of forward and reverse primers to amplify the breakpoint junctions on the two derivatives. The two breakpoints were located in nonhomologous regions, involving repetitive elements: MER4/AluJ on chromosome 8 and SVA element on chromosome X (Supplement figure 2). A segment of 88 bp was lost on the X chromosome in the translocation.

The translocation interrupted the *PTK2* gene at 8q24.3 in the 5'-UTR between exons 1 and 2, ~30 kb from the transcription start site, whereas no known gene was interrupted at Xq25. However, the transcription start site of the closest gene, *THOC2*, lay only 2 kb downstream of the breakpoint (see scheme in Fig. 1E).

PTK2 and THOC2 gene expression analyses

We initially evaluated *PTK2* gene expression by mRNA and protein analysis. (i) We showed that the rs7460 SNP, heterozygous in the patient's genomic DNA, was expressed only from the paternal allele (Fig. 2A). Real-time PCR on total RNA from fibroblasts showed a half-dose of the *PTK2* gene in the patient (0.5 ± 0.05, mean ± S.D.) compared to normal controls (1.0 ± 0.1, mean ± S.D., $p < 0.001$) (Fig. 2B). Western blot confirmed protein reduction in the patient (0.7 ± 0.1, mean ± S.D.) vs. controls (1.0 ± 0.05, mean ± S.D.) (Fig. 2C).

THOC2 showed an apparent mRNA overexpression (patient = 2.8 ± 0.025, mean ± S.D., controls = 1 ± 0.06, $p < 0.001$) with a real-time PCR assay on exons 33-34 from patient's fibroblasts (Fig. 2D). However, using an assay on exons 1-2 of the *THOC2* gene revealed a transcript reduction to about half the dose of controls (patient= 0.5 ± 0.035, mean ± S.D.; controls = 1 ± 0.06, $p < 0.01$) (Fig. 2D)

THOC2 protein levels were also significantly reduced (patient = 0.4 ± 0.1, mean ± S.D., controls = 1 ± 0.9, $p < 0.01$, two-tailed Student's t-test) (Fig.2E).

To test the effect of the translocation on *THOC2* flanking genes, we measured the expression of *GRIA3* (patient= 0.97±0.04, controls= 1 ± 0.05, mean ± S.D.) and *XIAP* (patient 0.93 ± 0.10, controls 1 ± 0.08, mean ± S.D.) vs. *TBP* in the patient's fibroblasts. Expression of both genes was similar to controls.

We reasoned that even if the breakpoint on the der(X) lay outside the *THOC2* coding sequence, it could alter *THOC2* expression by transcriptional interference.

PTK2-THOC2 fusion sterile transcript

The above results suggested that two different mRNAs were produced from the der(X): a less abundant, corresponding to the wild type transcript, initiated at the *THOC2* transcription start site (TSS), and a more abundant, fusion transcript under the control of the *PTK2* promoter. The fusion transcript was confirmed by RT-PCR on RNA from the patient's fibroblasts, using a forward primer within *PTK2* exon 1, and a reverse primer in *THOC2* exon 2 (Fig. 3A). The sequence of the PCR product showed the skipping of *THOC2* exon 1, likely because the first exon does not have an acceptor splice site (see scheme in Fig. 3A). The expected sterility of the fusion transcript was confirmed in vitro through a coupled transcription/translation assay: as shown in figure 3B, the 45.7 kDa protein produced in the control lane was absent in the transcribed and translated *PTK2-THOC2* construct (see also the supplement).

PTK2 promoter transcriptional interference on THOC2

To evaluate whether expression of the fusion transcript affected expression of the wild type *PTK2* allele, we treated the patient's fibroblasts with 50 ng/ml TNF-alpha for 6 hours, known to induce *PTK2* expression [11]. By real-time PCR, we measured expression of wild type *PTK2*, wild type *THOC2* (exons 1-2) and the sum of wild type *THOC2* and the fusion transcript (with an assay on *THOC2* exons 33-34). Under these conditions, wild type *PTK2* mRNA was significantly induced (untreated cells = 1 ± 0.032, mean ± S.D., treated cells = 1.5 ± 0.048, $p < 0.001$) (Fig. 3C). TNF-alpha also elicited a ~60% increase in expression of total *THOC2* mRNA (untreated cells 1 ± 0.037, mean ± S.D., treated cells 1.6 ± 0.084, $p<0.001$), but at the same time produced ~10% reduction of the wild type *THOC2* (untreated cells 1 ± 0.034, mean ± S.D., treated cells 0.9 ± 0.016, $p=0.0052$) (Fig. 3C).

Ptk2 and Thoc2 expression in mouse brain

To better interpret the results obtained in the patient's cells, we investigated *PTK2* and *THOC2* function in cellular and animal models.

We measured *Ptk2* and *Thoc2* mRNA expression in murine brain and cerebellum at different developmental stages (E14, P0, P60) (Fig. 4A, B). Expression of both genes seemed to increase from embryonic to adult life in the two tissues. It has been shown by *in situ* hybridization experiments, using an antisense probe, that

Thoc2 is highly expressed in brain, especially in the frontal cortex, and selectively expressed in the cerebellar region corresponding to the Purkinje cell layer (Fig. 4C, D Allen Institute for Brain Science. ©2009. http://mouse.brain-map.org, experiment 69444837).

Kin-32 and thoc-2 models in C. elegans

C. elegans has one *THOC2* homolog known as *thoc-2* or *tag-13*, and one *PTK2* homolog known as *kin-32*. *Kin-32* encodes, by alternative splicing, two isoforms of a focal adhesion kinase, orthologous to human *PTK2* and *PTK2B* [12]. Consistent with previous findings [12], we observed that *kin-32* knockout animals were viable, fertile and did not show anomalies in development, locomotion or chemosensory activity. On the other hand, *thoc-2* appears to be necessary for animal viability (www.wormbase.org). A strain containing a large, *thoc-2* homozygous, lethal deletion toward the C-terminus of the *thoc-2* gene (ok961) is therefore maintained as a balanced heterozygote with a *bli-4*- and GFP-marked translocation. *C. elegans thoc-2* knockouts (25%) were slow-growing, became sterile adults with vulve defects (www.wormbase.org) and died prematurely (*our unpublished observation*).

Animals *thoc-2*$^{+/+}$ (25%) were not viable due to segregation with the homozygous lethal *bli-4* balancer; *thoc-2*$^{+/-}$ were instead wild-type-looking animals, with normal fertility and slightly retarded development. Further experiments were therefore performed on *thoc-2*$^{+/-}$ and *thoc-2*$^{-/-}$ animals.

Animals *thoc-2*$^{-/-}$ were almost completely immobile, or moved slowly and for a short time upon touching. Locomotion was also statistically reduced in heterozygotes (Fig. 5A). On the other hand, mechanosensory neurons were not affected in either genotypes, as shown by a normal response to head and tail touch (data not shown). The chemotaxis index, tested in a mixed population of *thoc-2* knockouts and heterozygotes, was significantly reduced for different attractants / repulsive chemicals, proving a defect in specific sensory neurons (Fig. 5B).

Thoc2 knockdown in mouse LC-1 cells and in rat hippocampal cells.

The anatomical and functional abnormalities detected in the patient suggested that a reduced dosage of *THOC2* could determine specific abnormalities in the proliferation, differentiation and/or survival of neuronal precursor cells or in the survival of differentiated neurons. To address these possibilities, we conducted knockdown studies in rodent cells transfected with shRNA constructs capable of reducing the *Thoc2* ortholog expression by approximately 70% in HeLa cells (data not shown). To analyze the possible effects of *Thoc2* knockdown on the expansion of neuronal precursors we used mouse LC-1 cells, which are positive for the neuronal progenitor marker nestin and rapidly proliferate in presence of FGF2 and EGF, but

differentiate with high efficiency into neurons and astrocytes when cultured without growth factors [13]. On the other hand, to address the role of *Thoc2* in neuronal differentiation, we resorted to rat hippocampal neurons in primary culture [14]. These cells were transfected with shRNA constructs before plating and allowed to differentiate for ~72 hours. In both systems, *Thoc2* silencing did not increase significantly the number of apoptotic cells (data not shown), thus excluding that *Thoc2* knockdown affected neuronal cell viability. On the contrary, *Thoc2*-depleted LC-1 cells displayed a significantly increased proliferation rate, as determined by the MTT assay (Fig. 6A). In differentiating primary hippocampal neurons, the knockdown of *Thoc2* produced a significant increase in the length of neuronal processes (Fig. 6B-C), without affecting the timing of transitions between the first differentiation stages (data not shown).

DISCUSSION

Chromosomal rearrangements have been instrumental in identifying disease-causing genes located across or near the breakpoints [15, 16]. Here we describe a *de novo* reciprocal translocation between Xq25-ter and 8q24.3-ter, associated with psychomotor retardation and congenital cerebellar hypoplasia, likely caused by altered expression of two genes, *PTK2* at 8q24.3 and *THOC2* at Xq25.

The 8q24.3 breakpoint occurred within the *PTK2* gene. As expected, the mRNA and PTK2 protein levels were reduced to 50% in the patient's fibroblasts, compared to healthy controls. The absence of mutation in the transcript expressed by the second *PTK2* allele does not support the hypothesis of a recessive phenotype. *PTK2* encodes a cytosolic protein tyrosine kinase involved in focal adhesion formation [17]. Its activity elicits intracellular signal transduction pathways that stimulate the turn-over of cell contacts with the extracellular matrix, promoting cell migration. PTK2 has been implicated in central nervous system development and myelination, and synaptic plasticity in the mouse hippocampus [18, 19, 20].

Although we cannot exclude that *PTK2* haploinsufficiency played some role in our patient's phenotype, it is worth noting that: (a) micro- and macro-deletions (~120 kb to 6.9 Mb) containing *PTK2* have been reported in at least two healthy parents of children with cognitive impairment, with or without malformations (ref: #255112 Decipher Database; #11255_85 Rome, Italian Database of Copy Number Variants, http://dbcnv.oasi.en.it); (b) *Ptk2* homozygous knockout is lethal in mice, whereas haploinsufficiency does not result in a pathological phenotype [21]. Purkinje cells from homozygous conditional knockout mice show a normal phenotype [22]; (c) *kin-32* (*PTK2* ortholog) silencing in *C. elegans* did not affect viability, development, fertility, locomotion and chemosensory activity.

The Xq25 translocation created a fusion product which maintained both the *PTK2* and *THOC2* promoters. We demonstrated that the transcription of the *PTK2 – THOC2* fusion gene, under the *PTK2* promoter, downregulates the level of the wild type *THOC2* mRNA and protein.

Such a phenomenon, known as transcriptional interference [23], is responsible of a variety of human diseases, e.g., alpha-thalassemia (a gain-of-function, regulatory single-nucleotide polymorphism creates a new promoter-like element that interferes with normal activation of all downstream alpha-like globin genes [24]); Lynch syndrome: *TACSTD1* – a gene upstream to the Mismatch repair *MSH2* gene, transcribed in the same direction – not rarely shows deletions spanning the last exon, including the polyA signal. The RNA polymerase proceeds, interfering with the transcription of the downstream *MSH2* promoter, and gives rise to *TACSTD1/MSH2* fusion transcripts [25].

THOC2 product is a subunit of a multiprotein complex called the THO complex, which is conserved from yeast to humans [26]. THO interacts physically and functionally with the mRNA export factors Yra1 and Sub2 forming the TREX (TRanscription-EXport) complex.

It has been shown that TREX plays a role in mRNA transport from the nucleus to cytoplasm and distinct pathophysiological states are correlated with defective mRNA export mechanisms [27]. *Thoc5* deletion in mice causes death in the first two weeks after birth, similar to *Thoc1* deletion. *Thoc5* conditional knockout mouse developes acute leukocytopenia and anemia, suggesting that the TREX complex has a key role not only in early embryogenesis, but also in differentiation, as previously reported with *Thoc1* knockout [28, 29]. Other mRNA export genes have been linked to human diseases, such as the fragile X mental retardation protein, FMRP, that regulates mRNA metabolism and translation of key molecules involved in receptor signalling and spine morphology [30].

THOC2 is expressed in murine brain, and its pattern in the cerebellum is compatible with Purkinje cells distribution, consistent with our patient's clinic-pathological phenotype. *PTK2* is also expressed in brain, but with a more diffuse pattern [22]. In the cerebellum, the generation of the different categories of neurons is accomplished through well-defined space and time constraints, regulated by signals which are only partially known [31]: downregulation of *THOC2*, possibly combined with *PTK2* haploinsufficiency, may lead to aberrant timing of axonal sprouting or altered proliferation of specific neuronal populations, thus determining the cerebellar hypoplasia/cognitive impairment found in our patient.

Indeed, using fibroblasts from our patient, we demonstrated that when the *PTK2* gene was upregulated by TNF-alpha, the fusion transcript was overexpressed, whereas wild type *THOC2* gene was further repressed. We suggest that *THOC2* downregulation by transcriptional interference is a hypomorphic mutation and its expression may be further reduced in tissues where the ratio *PTK2/THOC2* favors the former.

The possible role of *THOC2* in the pathogenesis of our patient's phenotype was supported by our findings in three cellular/animal models: (i) *thoc-2* gene knockout in *C.elegans* were almost completely immobile and *thoc-2*$^{+/-}$ had impaired locomotion activity. The function of sensory neurons (AWA, AWB, AWC, ASE) was significantly impaired even in a mixed population of heterozygotes and *thoc2* knockouts. (ii) In LC1 mouse

neuronal precursors, downregulated *Thoc2* (~30% of the wild type) led to a significant increase in the proliferation, and (iii) in rat hippocampal primary neurons an increased length of neurites.

Overall, these data prove a neuronal defect driven by *THOC2* suppression and suggest that *THOC2* is a dosage-sensitive gene. Thus, *THOC2* may represent a further member of nuclear mRNA export factors, whose inappropriate interaction, expression pattern and possibly mRNA-binding specificity are expected to produce a variety of congenital syndromes, associated with brain diseases.

In conclusion, we describe a female with a cerebellar hypoplasia-psychomotor delay syndrome in which a chromosomal translocation alters the expression of two genes, *PTK2* and *THOC2*, involved in central nervous system. Our data and that of the literature suggest that the phenotype in our patient is due to the decreased expression of *THOC2*, or to a combined effect of *THOC2/PTK2* reduction, although no definitive evidence exists in support of one of these two hypotheses.

ACKNOWLEDGMENTS

We are gratefully indebted to the family who participated in this study. This work was supported by, the VERUM foundation, the French Association Connaitre les Syndromes Cérébelleux, the National Ataxia Foundation, the "Associazione E.E. Rulfo per la Genetica Medica", and A.I.S.A. Piemonte. NV is recipient of "My First Airc Grant" (MFAG11509). The funding organizations had no role in study design, data collection and analysis, decision to publish, or preparation of the manuscript. We thank the clinicians who referred their patients, the technical assistance of Dr. P. Pappi (Medical Genetics Unit, A.O. Città della Salute e della Scienza, Turin, Italy), Drs. E. Ferrero and Nicola Migone (University of Turin) for her advice and critical reading of the manuscript, and all members of the DNA and Cell bank team of the Centre de Recherche de l'Institut du Cerveau et de la Moelle épinière (Paris, France). LC1 neural stem cells were a kind gift from Luciano Conti (Department of Pharmacological Science, University of Milan, Milan, Italy).

FIGURE LEGENDS

Figure 1. Patient's MRI, karyotype, X-inactivation and FISH analysis.

(A) T1-weighted magnetic resonance imaging of the patient at 6 yrs showed hypoplasia of the cerebellar vermis, with enlargement of the IV ventricle and cisterna magna (see also supplement figure 1). (B) A translocation involving chromosome bands Xq25 and 8q24 was initially identified in the patient by standard karyotype. (C) X-inactivation analysis in the patient using the "humara test" showed a completely skewed pattern. (D) FISH analysis using two representative probes, one for chromosome 8 (RP11-159E16) and one for chromosome X (RP5-931E15) revealed the two derivatives and allowed definition of the breakpoint region. (E) Schematic representation of the Xq25 and 8q24.3 regions involved in the translocation. Genes are indicated as white or coloured boxes. The gene name is followed by a symbol indicating transcription direction. FISH probes used to define the breakpoint interval are indicated as grey bars. The breakpoint within the *PTK2* gene is enlarged.

Figure 2. Expression analysis of *PTK2* and *THOC2* genes in patient's cells.

(A) Sequence analysis of patient's genomic DNA (gDNA) and cDNA at SNP rs7460 in exon 32 of the *PTK2* gene. Only the maternal "T" allele was expressed. (B) Real-time PCR on the patient's cDNA extracted from fibroblasts showed a reduction of the *PTK2* gene measured vs. *TBP* reference (***$p<0.001$). (C) Reduction was confirmed at protein level vs. beta actin (ACTB) (**$p<0.01$). (D) Expression analysis of the *THOC2* gene (assay on exons 1-2) showed a ~50% reduction (reference gene *TBP*). However, using an assay on the 3'-end of the gene, *THOC2* transcript is apparently increased (***$p<0.001$, assay on exons 33-34). (E) *THOC2* reduction was confirmed at protein level vs. beta actin (ACTB) (**$p<0.01$). Statistic analysis was performed using a two-tailed Student's t-test.

Figure 3. *PTK2-THOC2* fusion transcript.

(A) The translocation juxtaposed *PTK2* to *THOC2* in the same transcriptional orientation (arrows). The *PTK2* promoter transcribed the *THOC2* gene; splicing generated a fusion transcript that lacks *THOC2* exon 1 (arrows indicate primers position to amplify the fusion transcript). (B) Coupled in vitro transcription/translation of a plasmid containing the fusion transcript (*PTK2* exon 1-*THOC2* exon 1-12) and a control insert (*THOC2* exons 1-12) showed that no internal translation start site is used by the fusion transcript, which did not code. The expected weight of the THOC2 wt protein coded by exons 1 to 12 is 45.7

kDa. (C) Six hours treatment with 50 ng/ml of TNF-alpha induced *PTK2* mRNA expression in fibroblasts from the patient. Real-time PCR showed an increase of the *PTK2* (untreated cells 1 ± 0.032, mean ± S.D., treated cells 1.5 ± 0.048, ***p<0.001) and *PTK2-THOC2* fusion product (assay on exons 33-34) expression (untreated cells 1 ± 0.037, mean ± S.D., treated cells 1.6 ± 0.084, ***p<0.001) relative to *TBP*. A reduction of *THOC2* expression vs. *TBP* was shown by real-time PCR assay on exon 1-2 (untreated cells 1 ± 0.034, mean ± S.D., treated cells 0.9 ± 0.016, **p=0.0052). Statistic analysis was performed using a two-tailed Student's t-test. UT: untreated cells; TSS: Transcription Start Site.

Figure 4. Expression analysis of *Ptk2* and *Thoc2* in mouse brain.

(A)–(B) Expression analysis of *Ptk2 and Thoc2* genes vs. *Hmbs* in murine brain or cerebellar lysates by real-time RT-PCR, at different developmental stages (E14, P0, P60). *Ptk2* and *Thoc2* increased their expression during mouse development (brain from E14 to P60; cerebellum from P0 to P60) . (C) *Thoc2 in situ* hybridization (above Nissl, and below *Thoc2 In Situ* Hybridisation (ISH) expression highlighted) in adult mouse brain shows that the gene is highly expressed, with a prevalence in frontal cortex and cerebellum. In this last tissue, the pattern is compatible with Purkinje neurons (see enlargement in panel D)(Allen Institute for Brain Science. ©2009. Available from: http://mouse.brain-map.org).

Figure 5. Characterization of *C. elegans* neuronal features.

(A) Locomotion activity (body bends) in wild type, *thoc-2*$^{+/-}$ and *thoc-2*$^{-/-}$ one day-old adult animals, and (B) sensory function (chemotaxis index). The functionality of a specific subset of animal sensory neurons (AWA, AWB, AWC, ASE) was assessed by quantifying their attraction or repulsion to specific chemicals (respectively: pyrazine, nonanone, benzaldheide, NH_4Acetate). Bars represent mean of data coming from two to four independent experiments, each time carried in duplicate from two independent operators; error bars represent standard error of the mean (SEM); *p<0.05, ***p<0.001, two-tailed, unpaired Student's t-test.

Figure 6. *Thoc2* knockdown in LC1 neural precursor cells and rat hippocampal neurons.

(A) *Thoc2* knockdown stimulated the proliferation of LC1 neural precursor cells in culture. Neural precursor LC1 were electroporated with a scramble shRNA (shCTRL) or with specific shRNA expressing plasmid (sh2113) before plating, and allowed to proliferate in culture for 24h, 48h and 72h. The proliferation rate was measured using the MTT assay. *Thoc2* knockdown neurons grew faster than control cells (p<0.05, two-tailed, paired Student's t-test). (B-C) Primary rat hippocampal neurons were electroporated before plating

with control (shCTRL) or specific shRNA-expressing plasmids (sh8137, sh2113) and allowed to differentiate for three days. The knockdown of *Thoc2* gene stimulated neurite outgrowth (*$p<0.05$, **$p<0.01$, ***$p<0.001$, two-tailed, unpaired Student's t-test). Green signal in the transfected cells is GFP and red signal is the staining for Alpha-Tubulin (C).

REFERENCES

1 Steinlin M. Non-progressive congenital ataxias. *Brain Dev* 1998;**20**(4):199-208.

2 Manto MU, Jissendi P. Cerebellum: links between development, developmental disorders and motor learning. *Front Neuroanat* 2012;**6**:1.

3 Courchesne E, Townsend J, Akshoomoff NA, Saitoh O, Yeung-Courchesne R, Lincoln AJ, James HE, Haas RH, Schreibman L, Lau L. Impairment in shifting attention in autistic and cerebellar patients. *Behav Neurosci* 1994;**108**(5):848-65.

4 Zanni G, Bertini ES. X-linked disorders with cerebellar dysgenesis. *Orphanet J Rare Dis* 2011;**6**:24.

5 Zanni G, Saillour Y, Nagara M, Billuart P, Castelnau L, Moraine C, Faivre L, Bertini E, Durr A, Guichet A, Rodriguez D, des Portes V, Beldjord C, Chelly J. Oligophrenin 1 mutations frequently cause X-linked mental retardation with cerebellar hypoplasia. *Neurology* 2005;**65**(9):1364-9.

6 Illarioshkin SN, Tanaka H, Markova ED, Nikolskaya NN, Ivanova-Smolenskaya IA, Tsuji S. X-linked nonprogressive congenital cerebellar hypoplasia: clinical description and mapping to chromosome Xq. *Ann Neurol* 1996;**40**(1):75-83.

7 Bertini E, des Portes V, Zanni G, Santorelli F, Dionisi-Vici C, Vicari S, Fariello G, Chelly J. X-linked congenital ataxia: a clinical and genetic study. *Am J Med Genet* 2000;**92**(1):53-6.

8 Zanni G, Bertini E, Bellcross C, Nedelec B, Froyen G, Neuhauser G, Opitz JM, Chelly J. X-linked congenital ataxia: a new locus maps to Xq25-q27.1. *Am J Med Genet A* 2008;**146A**(5):593-600.

9 Stiernagle T. Maintenance of C. elegans. *WormBook* 2006:1-11.

10 Ventura N, Rea SL, Schiavi A, Torgovnick A, Testi R, Johnson TE. p53/CEP-1 increases or decreases lifespan, depending on level of mitochondrial bioenergetic stress. *Aging Cell* 2009;**8**(4):380-93.

11 Kurenova E, Xu LH, Yang X, Baldwin AS, Jr., Craven RJ, Hanks SK, Liu ZG, Cance WG. Focal adhesion kinase suppresses apoptosis by binding to the death domain of receptor-interacting protein. *Mol Cell Biol* 2004;**24**(10):4361-71.

12 Cram EJ, Fontanez KM, Schwarzbauer JE. Functional characterization of KIN-32, the Caenorhabditis elegans homolog of focal adhesion kinase. *Dev Dyn* 2008;**237**(3):837-46.

13 Conti L, Pollard SM, Gorba T, Reitano E, Toselli M, Biella G, Sun Y, Sanzone S, Ying QL, Cattaneo E, Smith A. Niche-independent symmetrical self-renewal of a mammalian tissue stem cell. *PLoS Biol* 2005;**3**(9):e283.

14 Banker G, Goslin K. Developments in neuronal cell culture. *Nature* 1988;**336**(6195):185-6.

15 Billuart P, Bienvenu T, Ronce N, des Portes V, Vinet MC, Zemni R, Carrie A, Beldjord C, Kahn A, Moraine C, Chelly J. Oligophrenin 1 encodes a rho-GAP protein involved in X-linked mental retardation. *Pathol Biol (Paris)* 1998;**46**(9):678.

16 Najm J, Horn D, Wimplinger I, Golden JA, Chizhikov VV, Sudi J, Christian SL, Ullmann R, Kuechler A, Haas CA, Flubacher A, Charnas LR, Uyanik G, Frank U, Klopocki E, Dobyns WB, Kutsche K. Mutations of CASK cause an X-linked brain malformation phenotype with microcephaly and hypoplasia of the brainstem and cerebellum. *Nat Genet* 2008;**40**(9):1065-7.

17 Andre E, Becker-Andre M. Expression of an N-terminally truncated form of human focal adhesion kinase in brain. *Biochem Biophys Res Commun* 1993;**190**(1):140-7.

18 Beggs HE, Schahin-Reed D, Zang K, Goebbels S, Nave KA, Gorski J, Jones KR, Sretavan D, Reichardt LF. FAK deficiency in cells contributing to the basal lamina results in cortical abnormalities resembling congenital muscular dystrophies. *Neuron* 2003;**40**(3):501-14.

19 Rico B, Beggs HE, Schahin-Reed D, Kimes N, Schmidt A, Reichardt LF. Control of axonal branching and synapse formation by focal adhesion kinase. *Nat Neurosci* 2004;**7**(10):1059-69.

20 Monje FJ, Kim EJ, Pollak DD, Cabatic M, Li L, Baston A, Lubec G. Focal adhesion kinase regulates neuronal growth, synaptic plasticity and hippocampus-dependent spatial learning and memory. *Neurosignals* 2012;**20**(1):1-14.

21 Ilic D, Furuta Y, Kanazawa S, Takeda N, Sobue K, Nakatsuji N, Nomura S, Fujimoto J, Okada M, Yamamoto T. Reduced cell motility and enhanced focal adhesion contact formation in cells from FAK-deficient mice. *Nature* 1995;**377**(6549):539-44.

22 Watanabe F, Miyazaki T, Takeuchi T, Fukaya M, Nomura T, Noguchi S, Mori H, Sakimura K, Watanabe M, Mishina M. Effects of FAK ablation on cerebellar foliation, Bergmann glia positioning and climbing fiber territory on Purkinje cells. *Eur J Neurosci* 2008;**27**(4):836-54.

23 Palmer AC, Egan JB, Shearwin KE. Transcriptional interference by RNA polymerase pausing and dislodgement of transcription factors. *Transcription* 2011;**2**(1):9-14.

24 De Gobbi M, Viprakasit V, Hughes JR, Fisher C, Buckle VJ, Ayyub H, Gibbons RJ, Vernimmen D, Yoshinaga Y, de Jong P, Cheng JF, Rubin EM, Wood WG, Bowden D, Higgs DR. A regulatory SNP causes a human genetic disease by creating a new transcriptional promoter. *Science* 2006;**312**(5777):1215-7.

25 Kovacs ME, Papp J, Szentirmay Z, Otto S, Olah E. Deletions removing the last exon of TACSTD1 constitute a distinct class of mutations predisposing to Lynch syndrome. *Hum Mutat* 2009;**30**(2):197-203.

26 Reed R, Cheng H. TREX, SR proteins and export of mRNA. *Curr Opin Cell Biol* 2005;**17**(3):269-73.

27 Rondon AG, Jimeno S, Aguilera A. The interface between transcription and mRNP export: from THO to THSC/TREX-2. *Biochim Biophys Acta* 2010;**1799**(8):533-8.

28 Mancini A, Niemann-Seyde SC, Pankow R, El Bounkari O, Klebba-Farber S, Koch A, Jaworska E, Spooncer E, Gruber AD, Whetton AD, Tamura T. THOC5/FMIP, an mRNA export TREX complex protein, is essential for hematopoietic primitive cell survival in vivo. *BMC Biol* 2010;**8**:1.

29 Wang X, Chinnam M, Wang J, Wang Y, Zhang X, Marcon E, Moens P, Goodrich DW. Thoc1 deficiency compromises gene expression necessary for normal testis development in the mouse. *Mol Cell Biol* 2009;**29**(10):2794-803.

30 Bagni C, Tassone F, Neri G, Hagerman R. Fragile X syndrome: causes, diagnosis, mechanisms, and therapeutics. *J Clin Invest* 2012;**122**(12):4314-22.

31 Carletti B, Williams IM, Leto K, Nakajima K, Magrassi L, Rossi F. Time constraints and positional cues in the developing cerebellum regulate Purkinje cell placement in the cortical architecture. *Dev Biol* 2008;**317**(1):147-60.

SUPPLEMENTARY MATERIALS AND METHODS

Cytogenetic, Fluorescence In Situ Hybridization (FISH) Analyses

G-banded metaphase chromosomes were analyzed at 550-band resolution. To map the breakpoints on chromosomes 8 and X by FISH, a series of bacterial artificial chromosomes (BAC) and P1 artificial chromosomes (PAC) clones were selected from the UCSC Genome Browser (http://genome.ucsc.edu, release NCBI36/hg18, March 2006) covering 8q24.3 (16 clones) and Xq24-25 (18 clones). BAC/PAC DNA was isolated using standard protocols. FISH probes were labelled, by nick translation (Roche Diagnostics, Mannheim Germany) with biotin-16-dUTP, and FISH-analyses were performed according to standard protocol.

Array-Comparative Genome Hybridisation (a-CGH)

Array-CGH was carried out on genomic DNA using a whole genome oligonucleotide microarray platform (Human Genome CGH Microarray 244A Kit; Agilent Technologies, Santa Clara, California, USA). This array consists of approximately 236,000 60-mer oligonucleotide probes with a spatial resolution of 8.9 Kb. Experiments were performed following manufacturer's instructions. Slides were scanned using a G2565BA scanner, and analyzed using Agilent CGH Analytics software ver. 4.0.81 (Agilent Technologies Inc.) with the statistical algorithm ADM-2 and a sensitivity threshold of 6.0. At least three consecutive probes had to be aberrant to be identified as significant copy-number change.

X-Inactivation Study

To determine X-inactivation pattern, a CAG triplet repeat in the first exon of the androgen receptor (*AR*) gene (Xq12) was analyzed by methylation-specific PCR as described [1]. The genomic DNA was amplified with and without prior Hae II methylation sensitive restriction enzyme digestion. Using a forward fluorescent labelled primer, we amplified the *AR* CAG-containing polymorphic region in the proband and her relatives, used as controls. Reaction products were electrophoresed on an ABI Prism 3100 Avant automatic sequencer (Applied Biosystems).

Breakpoint junction definition

To determine the boundaries of the breakpoint on chromosomes X and 8, we used a long range PCR strategy with various combinations of primers and the Expand Long Template PCR kit in the conditions specified

(Roche Diagnostics). The breakpoint junction on chromosome 8 was amplified using: 10 µM primers 5'-tcttctatttagtatttctgg and 5'-tgctgagaatgatggtttcc, 144 µM dNTPs, 1.8 mM $MgCl_2$, 90 ng of genomic DNA, and 1 U of Taq Gold (Applied Biosystems). The thermal cycling conditions were 7 min at 95°C, followed by 30 cycles 30 sec at 95°C, 30 sec at 51°C, 1 min at 72°C; a final extension of 10 min at 72°C. The breakpoint junction on chromosome X was amplified using: 10 µM primers 5'-ctgtgtctgtgtagaaagag and 5'-caggtgtggtaatgcatgcctggatc, 144 µM dNTPs, 2 mM $MgCl_2$, 40 ng of genomic DNA, and 1 U of Taq Gold (Applied Biosystems). The thermal cycling conditions were 7 min at 94°C, followed by 14 cycles 30 sec at 94°C, 30 sec at 62 - 0.5°C, 1 min at 72°C, 30 cycles 30 sec at 94°C, 30 sec at 55°C, 1 min at 72°C; a final extension of 10 min at 72°C. PCR products were purified using a ExoSAP strategy and directly sequenced by the Big-Dye cycle sequencing kit ver.1.1 and an ABI Prism 3100 Avant automatic sequencer (Applied Biosystems).

Expression analyses

Amplification of part of the *PTK2* cDNA was obtained using primers 5'-tattttgaagacttgagttatttcaga; 5'-gtgctctggtacaaagcatttctg under standard conditions. Patient was found heterozygous for the SNP rs#7460 in exon 32. TaqMan real-time quantitative PCR analysis was used to measure expression in human cells as follows: (a) *PTK2*, FAM-labeled pre-designed TaqMan gene expression assays (Hs00178587_m1, Applied Biosystems); (b) *THOC2* exons 1-2, primers 5'-caaggaatcttcagcaaagctc; 5'-ccatttctctctccttactcttgg; #68 probe (Roche Diagnostics); (c) *THOC2* exons 33-34, FAM-labelled pre-designed TaqMan gene expression assays (Hs00396154_m1, Applied Biosystem); (d) *XIAP*, FAM-labelled pre-designed TaqMan gene expression assays (Hs01597786_g1, Applied Biosystem); (e) *TBP* reference gene, VIC-labeled pre-designed TaqMan gene expression assays (Hs00427620_m1, Applied Biosystems). Reactions were carried out on an ABI 7500 Fast real-time PCR machine using the ABI TaqMan Universal PCR master mix according to the manufacturer's instructions (Applied Biosystems). Efficiencies of the assays were similar and in a range 90-110%. Patient, and three gender matched unrelated healthy controls were run in triplicate; the mean Ct value was used for calculations using the ΔΔCt method [2]. In situ hybridizations using antisense RNA in mouse brain, were obtained for *Thoc2* from "The Allen Brain Atlas" [3] (Allen Institute for Brain Science. ©2009. Available from: http://mouse.brain-map.org, experiment 69444837).

Western blot assay

Proteins from cell lysates (20 µg) were separated by precast gradient gel (4-15%) (Bio-Rad) and transferred to 0.45 µm nitrocellulose membrane (BIO-RAD). After blocking with 5% non-fat milk in Tris-buffered saline containing 0.1% Tween (TBS-T), protein blots were incubated with a specific antibody (PTK2, [4]

antibody against the C-terminus of THOC2 [5] and BACT (Novus Biological) followed by incubation with a peroxidase-conjugated secondary antibody in blocking buffer. Protein bands were visualized with the enhanced chemiluminescence method according to manufacturer's instructions (CYANAGEN).

Mice tissue collection and RNA isolation

The experimental protocol was approved by the Bioethical Committee of the University of Turin and by the Italian Ministry of Health. Mice were sacrificed under deep general anaesthesia (ketamine, 100 mg/kg; Ketavet, Bayern, Leverkusen, Germany; xylazine, 5 mg/kg; Rompun; Bayer, Milan, Italy). Brains were temporarily placed in an ice-cold artificial cerebro-spinal fluid containing 125 mM NaCl, 2.5 mM KCl, 2 mM $CaCl_2$, 1 mM $MgCl_2$, 1.25 mM NaH_2PO_4, 26 mM $NaHCO_3$, 20 mM glucose, bubbled with 95% O_2 and 5% CO_2. For the analysis on separated brains regions, cerebellums were manually dissected. All samples were rapidly frozen in 2-methylbutane and stored at -80°C. Total RNA was extracted with TRIzol Reagent (Invitrogen Life Technologies) in accordance with the manufacturer's instructions. One microgram of total RNA was reverse-transcribed using the High-Capacity cDNA Archive Kit (Applied Biosystem, Monza, Italy), accordingly to the manufacturer's instructions. cDNA samples were stored at -20°C.

TaqMan real-time quantitative PCR analysis was used to measure expression in mouse tissues using the following assays: *Thoc2*, primers 5'-gatctggccgaaataaccac; 5'-gcagttagaagccatgactg; UPL#46 human set probe (Roche Diagnostics); *Ptk2* primers 5'-gaaaagcggctgtagtcca; 5'-ccattcttttgctagatgctaggt UPL#70 human set probe (Roche Diagnostics); reference gene was *Hmbs* primers 5'-tccctgaaggatgtgcctac; 5'-cacaagggttttcccgttt; UPL#10 human set probe (Roche Diagnostics). Reactions were carried out and analysed as described above. Experiments were performed three times in triplicate.

In vitro transcription/translation

To obtain the chimeric *PTK2-THOC2* amplimer, we amplified the patient's cDNA using a forward primer on exon 1 of the *PTK2* gene (*T7 promoter* - specific primer, 5'-ggatcctaatacgactcactatagggagacc – accatggcggccgcggctgtgtgggttcccg) and a reverse primer on exon 12 of the *THOC2* gene (5'-ctccttcataaatgacttgcctatg). As control a *THOC2* partial transcript was obtained using primers in exon 1-exon 12 (*T7 promoter* - specific primer, 5'-ggatcctaatacgactcactatagggagacc - gcgtgaggcgtgggaggaagcgcgg). PCR conditions were: 200 nM of each primer, 200 μM dNTPs, 1x KAPA2G Buffer B, 100 ng of cDNA, and 1 U of KAPA2G Fast HotStart DNA Polymerase (KAPABiosystems). Transcription/translation was performed using TnT T7 Quick for PCR as described (Promega).

Caenorhabditis elegans models

C.elegans viability and development. The ability of animals to survive and develop to adulthood compared to a wild-type strain was assessed by scoring for three consecutive generations animals fed bacteria expressing empty-vector or bacteria expressing either of dsRNA against *kin-32* or *thoc-2*.

Fecundity/fertility. The total number of progeny (brood size or fecundity) and the number of eggs hatched (fertility) from three independent gravid adults (in two independent experiments) were scored in each of the above-described experimental conditions.

Sensory neurons functionality. Different types of chemosensory neurons respond to a variety of volatile and water-soluble chemicals. The functionality of a specific subset of animal sensory neurons (AWA, AWB, AWC, ASE) was assessed by quantifying their attraction or repulsion to specific chemicals (respectively: pyrazine, nonanone, benzaldheide, NH_4Acetate). Briefly, sodium azide (NaN_3) used to anesthetize worms is placed on buffered agar 180 degrees opposite on a 10 cm dish; the attractant (or repellent) is then placed on one NaN_3 spot, and ethanol (neutral odor for the worms in which attractant is diluted) on the other spot; a population of 80-100 age-synchronized animals are spotted in the centre of the testing plate and the number of worms at attractant and control are counted every 15 minutes for two hours to calculate the Chemotaxis Index (CI). CI=(A-B)/(A+B+C), where A is the number of worms at attractant, B is the number of worms at control and C is the number of animals which did not reach any of the two spots at the end of the two hours. For a population of young (3 days old), wild-type animals, a good CI is around 0,8 for attractants and –0.8 for repellents after two hours (CI=0 means no attraction, while CI=1 or –1 represent maximum attraction or repulsions, but there are always some animals that, also for a wild-type strain, remain randomly dispersed in the assay plate or reach the control spot instead of the attractant). *Che-3* sensory defective mutant was used as positive control.

Motoneuron activity. We calculated animal spontaneous locomotion counting the number of body bends (i.e., changes in the body bend at the mid-body point) per minute on solid agar plates with no bacteria. One bend was counted every time the mid-body reaches a maximum bend in the opposite direction from the bend last counted. Body bend was checked in at least 15 animals for 15 seconds.

Proprioception. Gentle touch to the body is sensed by touch receptor neurons, which extend their neurites in close contact with the cuticle along their entire length. In this assay animals were gently touched with an eyelash ten times, alternating six head (backward movement) and six tail (forward movement) touches, and a score was given for the number of positive responses. No more than six touches per side were done to avoid habituation.

All behavioral assays were performed on young animals on their first fertile day (3 day-old animals).

Plasmid preparation, transfections and silencing quantification

pGIPZ Lentiviral shRNAmir clones (Thermo Scientific, Open Biosystem) were grown for 18-19 hours at 37°C in LB broth media plus 100 μg/ml ampicillin. Plasmid DNA was extracted using Promega Pure Yield ™ Plasmid Miniprep System. We seeded $4 \cdot 10^4$ HeLa cells per well in 24-well plates and transfected them 24 h later with 500 ng of plasmid per well. Each plasmid was delivered using FuGene HD Transfection reagent (Roche) according to the manufacturer's protocol. Puromycin selection was done after 72 h using a puromycin working concentration of 3 μg/ml for 12 hours. Transfection efficiency was determined counting the percentage of fluorescent cells by flow cytometry using GFP-expressing plasmid . To analyze messenger RNA knockdown, cell were lysed and total RNA collected using the Cells-to-Ct kit (Applied Biosystem) in accordance with the manufacturer's protocol.

THOC2 mRNA level was determined by real-time RT-PCR as described above.

Mutation screening

Forty-two sporadic patients (33 males and 9 females) with mental retardation and childhood onset cerebellar ataxia were collected for mutation screening. PCR amplification and DHPLC analysis were performed as follow: *PTK2* and *THOC2* gene-coding regions were divided into 32 and 38 amplimers, respectively (sequences available upon request). Amplicons were run on DHPLC (Transgenomic WAVE System) using melting temperatures determined by the DHPLC Melt software (available upon request) [6]. A normal control profile was always compared with that from patient. For *THOC2*, two male patients were mixed to allow the formation of heteroduplexes. PCR products showing a DHPLC peak shift were purified using the ExoSAP system (Amersham-Pharmacia Biotech, Freiburg, Germany), and sequenced by the BigDye cycle sequencing kit and an ABI Prism 3100 Avant automatic sequencer (Applera). To determine whether a nucleotide change could affect splicing, we scored these substitutions by two web available softwares: the MaxENT (http://genes.mit.edu/burgelab/maxent//Xmaxentscan_scoreseq_acc.html)[7], and the Splice Site Prediction by Neural Network (http://www.fruitfly.org/seq_tools/splice.html) [8].

Whole gene deletions were screened using a real-time PCR assay centred on exons 3 for *PTK2* (conditions available upon request).

SUPPLEMENTARY RESULTS

Mapping of the translocation breakpoints by FISH

We performed FISH analysis on patient's metaphase spreads to characterize the breakpoint on both chromosome X and 8. We selected Bacterial Artificial Chromosomes (BACs) and P1 Artificial Chromosomes (PACs) . FISH analyses and clones that allowed the breakpoints identifications are reported in Fig. 1D and scheme 1E. On chromosome Xq24-25, we identified one PAC clone (RP5-931E15) hybridising both derivatives (Fig. 1D, 1E) and two flanking clones hybridising to chromosome X-der(X) (RP5-506G2), and chromosome X –der(8) (RP11-325K14). On chromosome 8q24 the breakpoint could be located in a region of ~ 33 kb overlapping two BAC clones (RP11-691F18 and RP11-159E16, Fig. 1D and E) which hybridised both derivatives (Fig. 1D).

Mutation analysis

With the aim of identifying a second patient with a mutation in *PTK2* or *THOC2* genes, we selected 42 pediatric cases (33 males and 9 females) with mental retardation and ataxia negative for mutations in known genes. The *PTK2* gene was screened in 18 patients (9 males and 9 females) by real time PCR for whole-gene deletions / duplications and by dHPLC for point mutations (see Table 1 in the supplement). All 42 cases were screened for *THOC2* point mutations by dHPLC (see Table 2 in the supplement). No mutation was detected in either screening.

SUPPLEMENT Figure1

Supplement figure 1. Patient's MRI at 15 months and 6 yr

T1-weighted magnetic resonance images of the patient at 15 months and 6 yr. Sagittal, axial and coronal sections showed cerebellar hypoplasia of the hemispheres and vermis with enlargement of the IV ventricle and cisterna magna.

Supplement figure 2. FISH analysis and sequences alignment at the two breakpoints

A) Schematic representation of the Xq25 and 8q24.3 regions involved in the translocation. Genes and their transcriptional orientation are indicated as dark grey arrows. FISH probes used to define the breakpoint

interval are indicated as grey bars. The breakpoint within *PTK2* and *THOC2* gene are enlarged. The repetitive elements MER4/AluJ on chromosome 8 and SVA on chromosome X were involved. B) Sequences alignment at the two breakpoints showed the involvement of nonhomologous regions and a 88 bp deletion at chromosome X.

REFERENCES

1 Kubota T, Nonoyama S, Tonoki H*, et al.* A new assay for the analysis of X-chromosome inactivation based on methylation-specific PCR. *Hum Genet* 1999;**104**(1):49-55.

2 Livak KJ, Schmittgen TD. Analysis of relative gene expression data using real-time quantitative PCR and the 2(-Delta Delta C(T)) Method. *Methods* 2001;**25**(4):402-8.

3 Lein ES, Hawrylycz MJ, Ao N*, et al.* Genome-wide atlas of gene expression in the adult mouse brain. *Nature* 2007;**445**(7124):168-76.

4 Retta SF, Barry ST, Critchley DR*, et al.* Focal adhesion and stress fiber formation is regulated by tyrosine phosphatase activity. *Exp Cell Res* 1996;**229**(2):307-17.

5 Masuda S, Das R, Cheng H*, et al.* Recruitment of the human TREX complex to mRNA during splicing. *Genes Dev* 2005;**19**(13):1512-7.

6 Jones AC, Austin J, Hansen N*, et al.* Optimal temperature selection for mutation detection by denaturing HPLC and comparison to single-stranded conformation polymorphism and heteroduplex analysis. *Clin Chem* 1999;**45**(8 Pt 1):1133-40.

7 Eng L, Coutinho G, Nahas S*, et al.* Nonclassical splicing mutations in the coding and noncoding regions of the ATM Gene: maximum entropy estimates of splice junction strengths. *Hum Mutat* 2004;**23**(1):67-76.

8 Reese MG, Eeckman FH, Kulp D*, et al.* Improved splice site detection in Genie. *J Comput Biol* 1997;**4**(3):311-23.

9 Goslin K, Banker G. Rapid changes in the distribution of GAP-43 correlate with the expression of neuronal polarity during normal development and under experimental conditions. *J Cell Biol* 1990;**110**(4):1319-31.

10 Ying QL, Smith AG. Defined conditions for neural commitment and differentiation. *Methods Enzymol* 2003;**365**:327-41.

Fig. 1

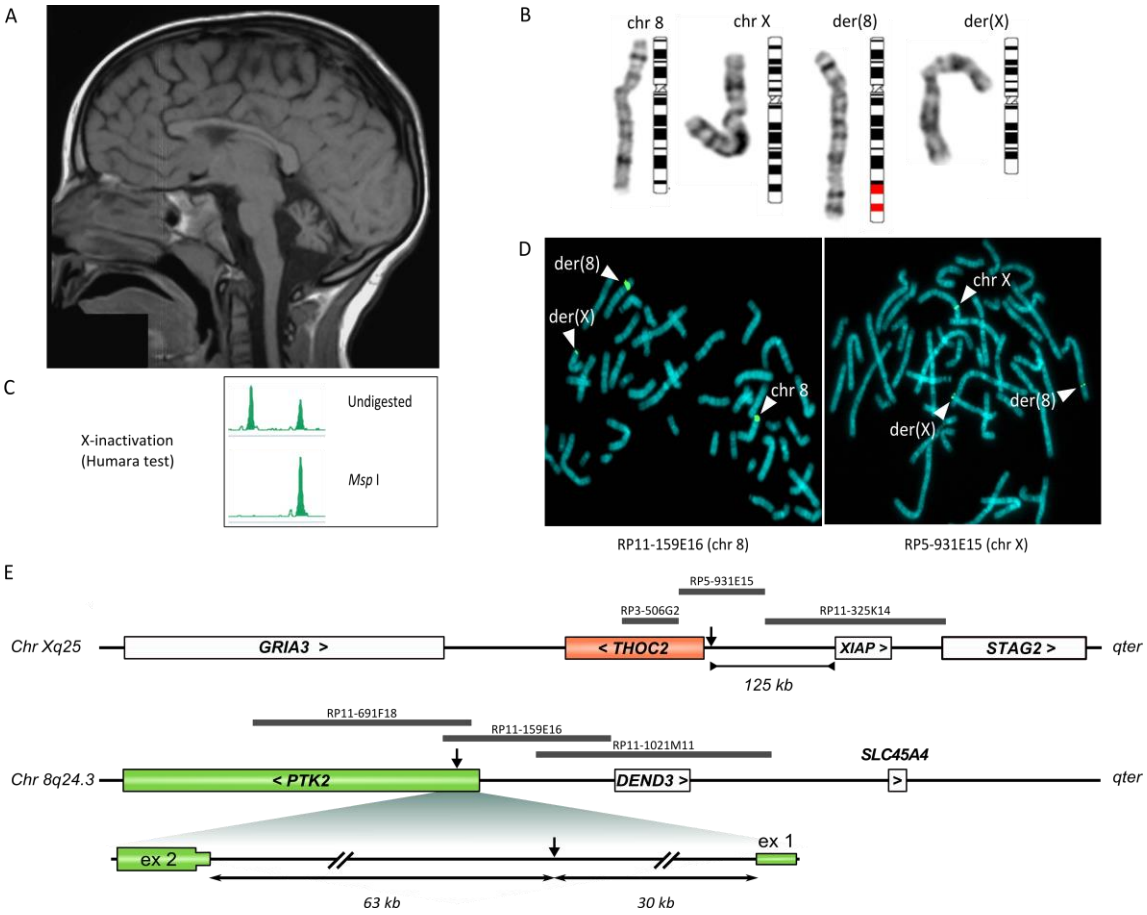
A
B
chr 8
chr X
der(8)
der(X)
C
X-inactivation
(Humara test)
Undigested
Msp I
D
der(8)
der(X)
chr 8
chr X
der(8)
der(X)
RP11-159E16 (chr 8)
RP5-931E15 (chr X)
E
RP5-931E15
RP3-506G2
RP11-325K14
Chr Xq25
GRIA3 >
< THOC2
XIAP >
STAG2 >
qter
125 kb
RP11-691F18
RP11-159E16
RP11-1021M11
SLC45A4
Chr 8q24.3
< PTK2
DEND3 >
>
qter
ex 2
ex 1
63 kb
30 kb

Fig.2

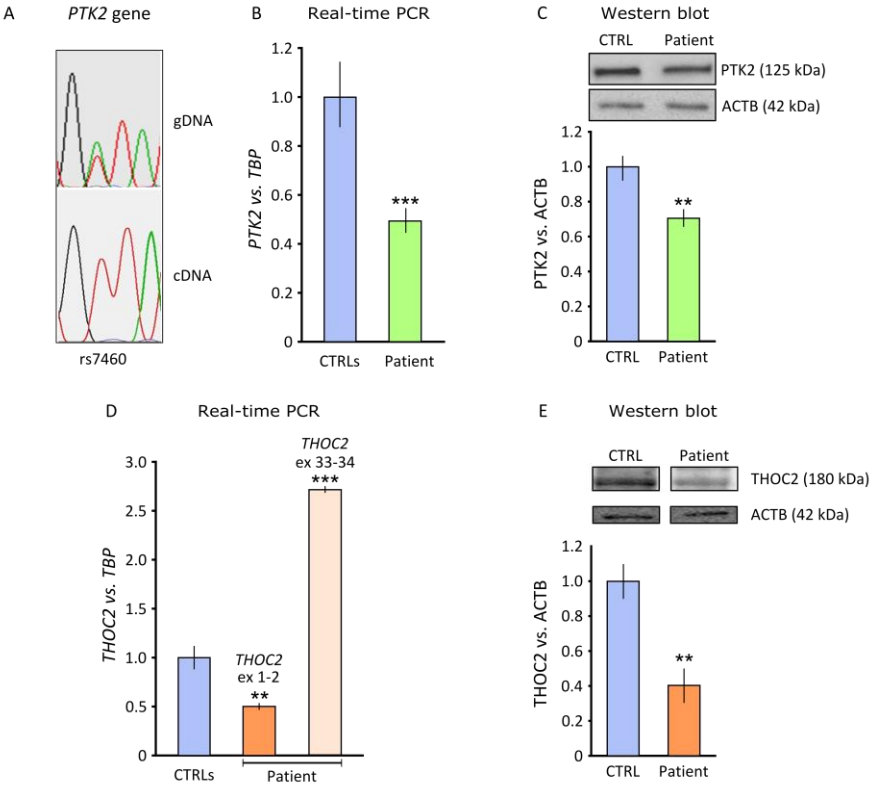
A
PTK2 gene
gDNA
cDNA
rs7460
B
Real-time PCR
PTK2 vs. TBP
CTRLs
Patient
C
Western blot
CTRL
Patient
PTK2 (125 kDa)
ACTB (42 kDa)
PTK2 vs. ACTB
D
Real-time PCR
THOC2 vs. TBP
THOC2 ex 33-34
THOC2 ex 1-2
E
Western blot
THOC2 (180 kDa)
ACTB (42 kDa)
THOC2 vs. ACTB

Fig. 3

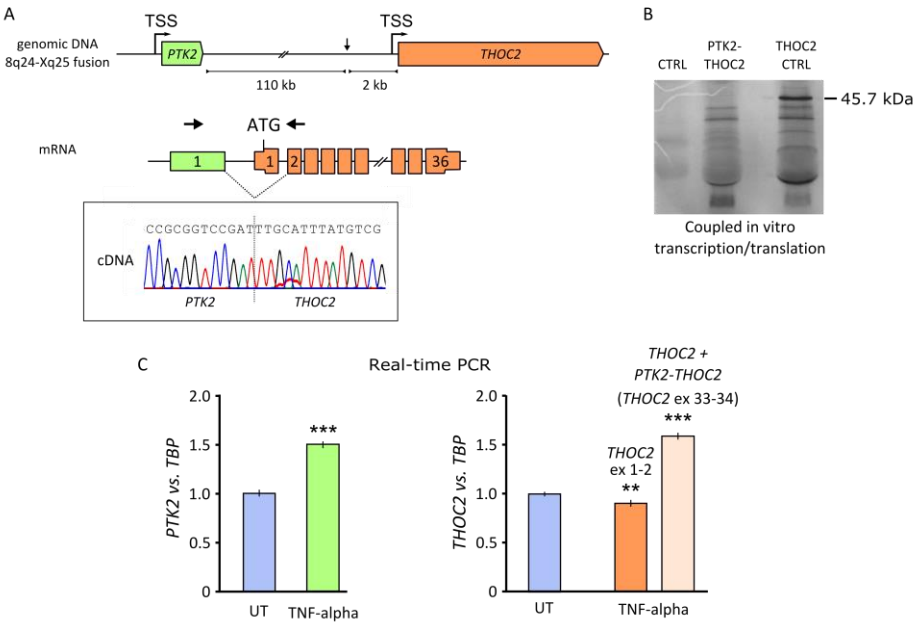
A
TSS
TSS
genomic DNA
8q24-Xq25 fusion
PTK2
THOC2
110 kb
2 kb
mRNA
ATG
1
1
2
36
CCGCGGTCCGATTTGCATTTATGTCG
cDNA
PTK2
THOC2
B
CTRL
PTK2-THOC2
THOC2 CTRL
45.7 kDa
Coupled in vitro transcription/translation
C
Real-time PCR
PTK2 vs. TBP
2.0
1.5
1.0
0.5
0
***
UT
TNF-alpha
THOC2 + PTK2-THOC2 (THOC2 ex 33-34)
THOC2 vs. TBP
THOC2 ex 1-2
**
***
UT
TNF-alpha

Fig. 4

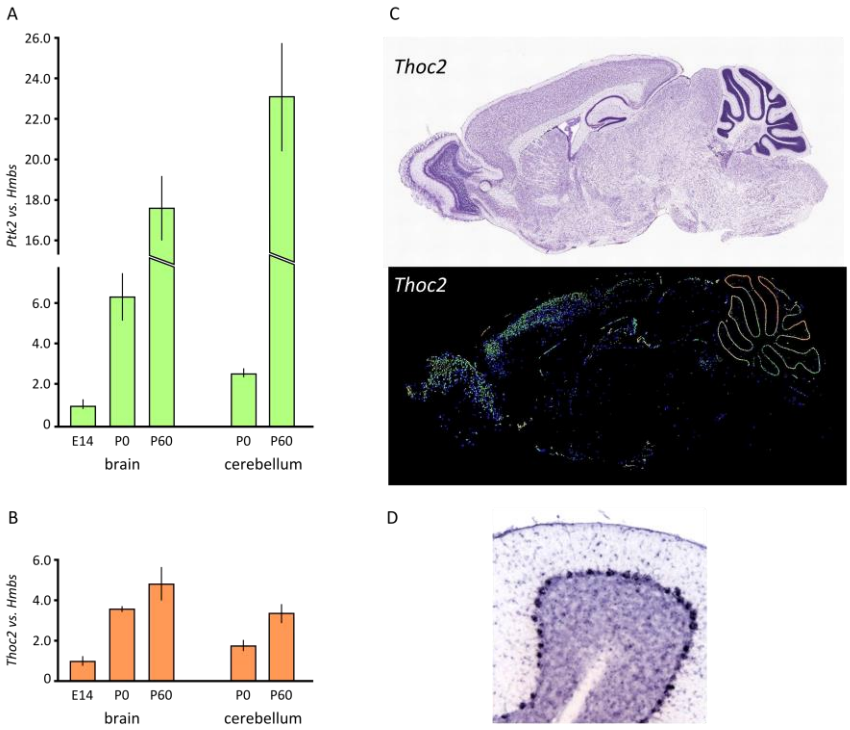
A
26.0
24.0
22.0
20.0
18.0
16.0
6.0
4.0
2.0
0
Ptk2 vs. Hmbs
E14
P0
P60
P0
P60
brain
cerebellum
B
6.0
4.0
2.0
0
Thoc2 vs. Hmbs
E14
P0
P60
P0
P60
brain
cerebellum
C
Thoc2
Thoc2
D

Fig. 5

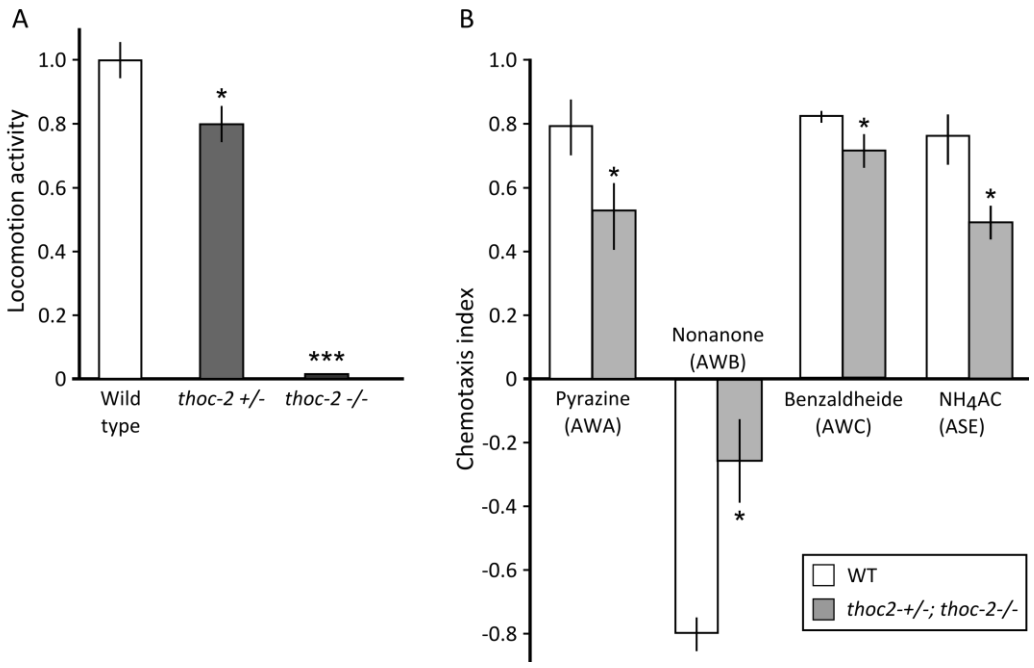
A
Locomotion activity
1.0
0.8
0.6
0.4
0.2
0
*
***
Wild type
thoc-2 +/-
thoc-2 -/-
B
Chemotaxis index
1.0
0.8
0.6
0.4
0.2
0
-0.2
-0.4
-0.6
-0.8
Pyrazine (AWA)
Nonanone (AWB)
Benzaldheide (AWC)
NH4AC (ASE)
WT
thoc2-+/-; thoc-2-/-

Fig. 6

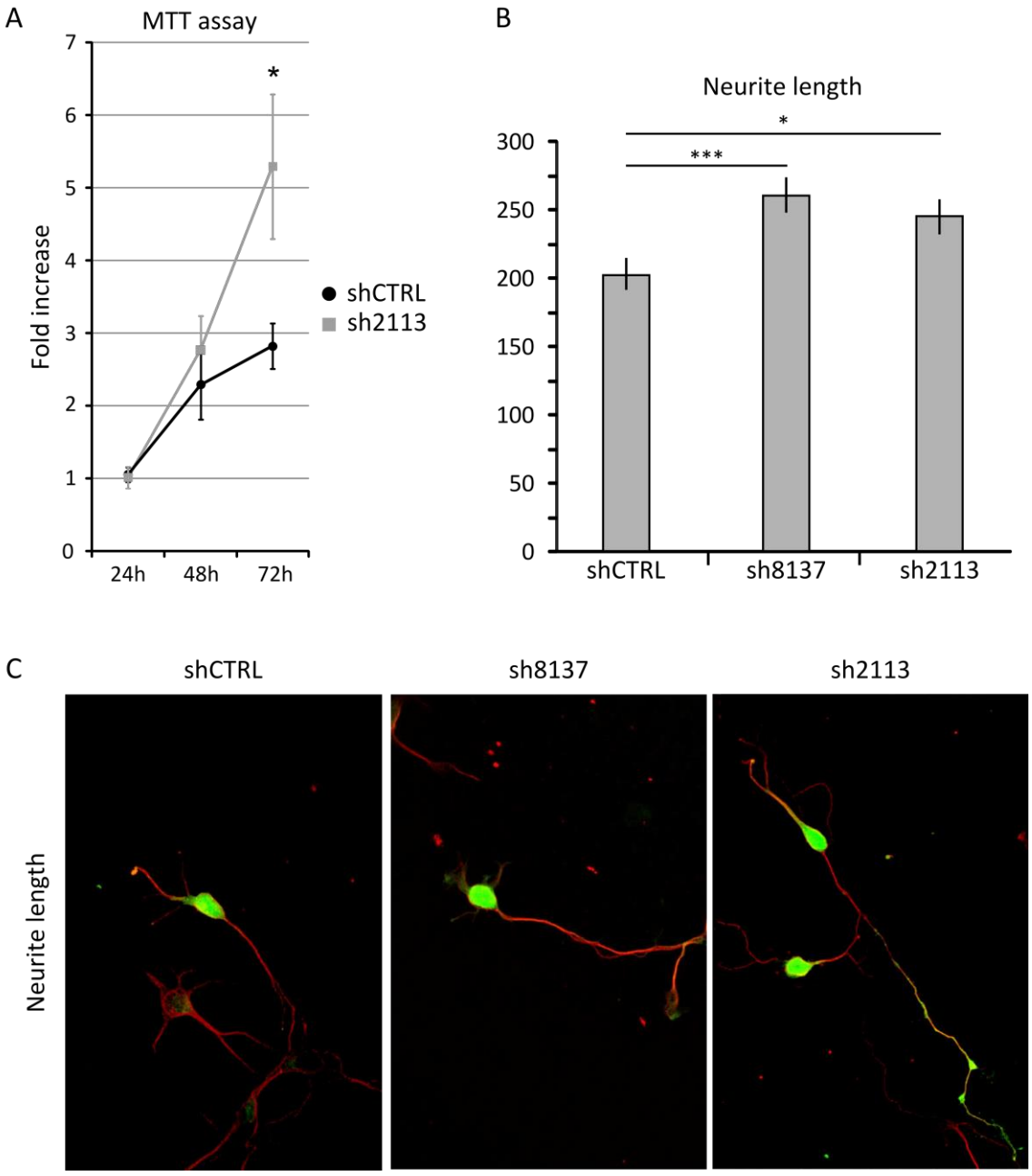
A
MTT assay
Fold increase
7
6
5
4
3
2
1
0
*
24h
48h
72h
shCTRL
sh2113
B
Neurite length
*
***
300
250
200
150
100
50
0
shCTRL
sh8137
sh2113
C
shCTRL
sh8137
sh2113
Neurite length

Supplemental fig. 1

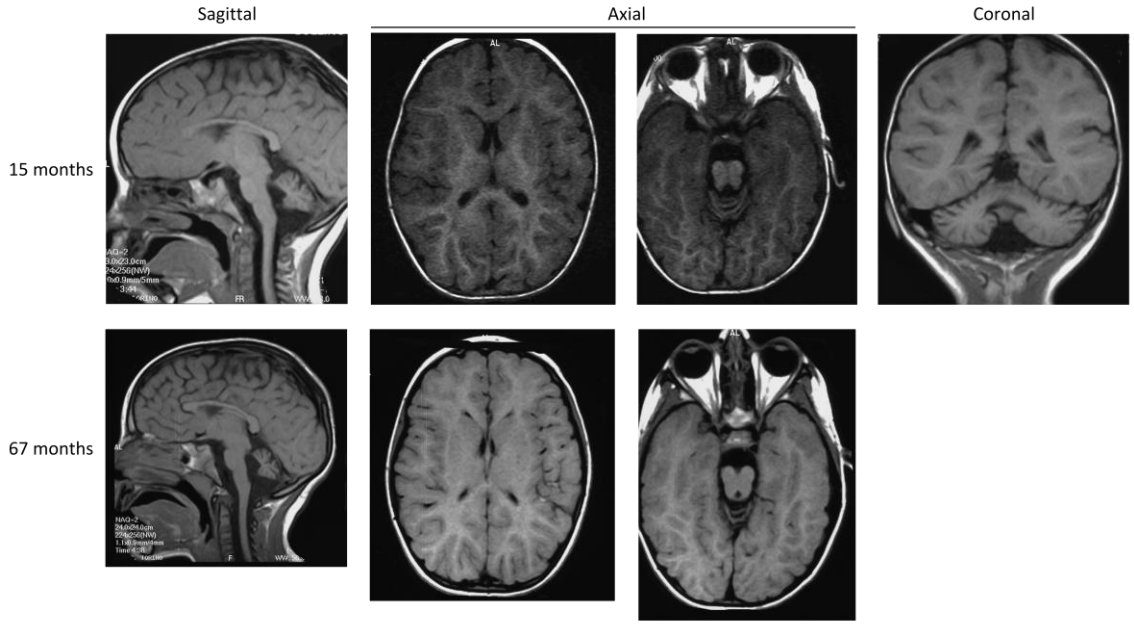

Figure S2